International Journal on Advanced Science Engineering Information Technology

Vol.12 (2022) No. 4
ISSN: 2088-5334

Stratified Two-Phase Turbulent Pipe Flow Simulations

Imad Taher Ali [a], Imran Afgan [a,b,*], Ilyas Khurshid [b]

[a] *Department of MACE, School of Engineering, The University of Manchester, M13 9PL, United Kingdom*
[b] *Mechanical Engineering Department, School of Engineering, Khalifa University, Abu Dhabi, P.O. Box 127788, UAE*
*Corresponding author: *imran.afgan@manchester.ac.uk*

***Abstract*—Gas-liquid two-phase flows in pipes are common in various industrial processes requiring fluid transport through pipes and ducts under varying operating conditions. Computational fluid dynamics (CFD) simulations of various conditions of gas-liquid turbulent flow in a horizontal circular pipe are presented in the current paper. The simulations utilize the Level-set Method coupled with the Volume of Fluid (VOF) method to calculate the normal interface for the VOF re-construction step. In the present approach, the flow governing equations are solved numerically first for the mixture, followed by an additional equation for the second phase. A geometric re-construction technique is then used to reconstruct the interface between the two phases. This geometric re-construction technique is based on a piece-wise-linear interface construction approach. For the simulations, a number of eddy viscosity models (EVM) were tested, namely, $k-\varepsilon$, $k-\omega$, and the Re-Normalisation Group (RNG) $k-\varepsilon$ in both standard and differential form of turbulence viscosity. Numerical results were validated against detailed measurements and mechanistic models and were found to be in complete agreement. The results were analyzed for the flow physics of the transfer of momentum across the stratified two-phase using the velocity profiles of the gas and liquid phases, liquid hold-up, and different hydrodynamic forces. The paper also highlights the suitability of such a coupled VOF approach for stratified flows via comparisons against measurements and common industrial mechanistic models.**

***Keywords*— Hydraulic gradient; turbulent pipe flow; stratified flow; two-phase flow; volume of fluid.**

Manuscript received 26 Aug. 2021; revised 4 Oct. 2021; accepted 24 Feb. 2022. Date of publication 31 Aug. 2022.

I. INTRODUCTION

Gas-liquid two-phase flows in pipes are quite common in various industrial processes such as oil and gas, chemical plants, hydro and nuclear power plants etc. Many of these sectors' processes require liquid transport through pipes and ducts under varying operating conditions. A stratified two-phase flow commonly appears at low liquid and gas flow rates where complete separation of the two phases occurs. Depending on the gas flow rate, the interface between the phases may appear smooth or wavy, introducing a subdivision of this pattern (i.e., stratified and stratified-wavy flow). The wavy stratified flow regime can be broadly categorized, based on the wave structures, into rippled, two-dimensional (2D), and roll waves [1]. In many stratified two-phase pipe flows, the estimation of primary design parameters, such as volumetric ratios, interfaces, pressure drop etc., is generally done through empirical correlations. However, most of these correlations' predictive capabilities seem to deteriorate when applied to flow conditions different from those used in their tuning [2]. A slightly more advanced way of modelling two-phase flows is by the use of the momentum balance mechanistic models. In such semi-empirical models, the pressure forces are balanced with the shear and gravitational forces using different shear force correlations which are necessary to close the model. However, these phenomenological or mechanistic models are also quite limited, due to their inability to account for the inherent unsteadiness in the flow [3]. The alternative is thus to use a mathematical modeling approach that can capture both the transition and the interface of such complex flow problems.

Early work aiming at employing the turbulent eddy viscosity hypothesis in the Computational Fluid Dynamics (CFD) simulations was mainly restricted to flows in rectangular cross-section ducts [4]. In these two-dimensional (2-D) studies, simple steady-state turbulence models were used for each of the two phases. In the majority of the cases, the interface was assumed to be smooth. On the other hand, for the wavy flow configuration, the interface was treated as a rough moving wall with an imposed interfacial roughness, estimated from the measurements of the relative height of

interface waves. Reasonable agreements were reported for measurements in simple channel flows.

For a slightly more complicated pipe flow geometry [5], the flow in the liquid phase was solved only with the gas phase treated as a bulk flow. Relatively simple turbulence models were used, and the phases were coupled by explicitly giving an empirical friction factor to calculate the interfacial shear stresses. The results compared well to the mechanistic model [6]. For the same problem, [4] used a slightly more advanced approach by solving both the phases with the assumption of a smooth interface, showing a good agreement with measurements. This approach was later used to recalculate the cases of [5]. However, comparisons with experiments showed large discrepancies. Using a low Reynolds model approach, this work was later extended to a larger pipe diameter [7], where the coupling between phases was achieved through the velocity, assuming equal shear stresses at the interface. [8] used a similar approach to simulate wavy stratified gas and liquid mixture flow through a pipe with an imposed interfacial roughness using algebraic models to account for the secondary flows. They successfully reproduced the experimental observations of [9]**Error! Reference source not found.**, which are of interest in the present study. These measurements were also numerically reproduced [10] but with a number of simplifications; they solved for the gas phase only by using an imposed roughness at the interface [9]. The pipe bottom wall was assumed as a rough moving flat surface. A high level of success was reported by simplifying the problem down to a single-phase flow.

Using only half of the pipe cross-section, various oil-gas two-phase flow regimes for different pipe orientations was simulated [11]. The VOF model was used to get qualitative results only with the assumption of laminar flow, which is not necessarily a true representation of the original problem [11]. More recently, the same approach was used but with the $k-\varepsilon$ turbulence model [12]. The simulated phases (air and water) were introduced as a mixture at the pipe inlet, similar to the scenario that is adopted in the present work. However, only qualitative comparisons were shown, which cannot be used to predict the accuracy and reliability of the presented model.

More recently, a number of studies have been conducted on two-phase flows with the use of sophisticated experimental and numerical techniques [13]–[24] and also by utilizing machine learning [25]–[38]. However, in the literature, most studies deal with either a specific flow regime or use many simplifications with or without empirical formulations (see [39]). Nevertheless, a few exceptions exist where a wider range of flow regimes is simulated, but the reported comparisons are only qualitative.

Furthermore, almost all the numerical approaches discussed till now require prior knowledge about either the position of the interface or the stresses on it. Thus, it seems that there are still a number of gaps when it comes to the CFD modeling of multi-phase flows in pipes. The present contribution presents a methodology that does not require any empirical information and in which the interface is tracked naturally through a transient solution of the flow governing equations. Thus, the current modeling approach is more robust as it does not require the simulated flow regime to be known a-priori.

II. Material and Method

A. The Volume-of-Fluid Model

Various numerical models have been developed to solve the governing equations and track the interface between the phases, including the well-known Volume of Fluid (VOF) model [40]. This model was developed for naturally coupling the two phases and tracking the interface between them. In the VOF model, a volume fraction function (α) is defined whose average value is unity (1) in any cell that is fully occupied by the liquid phase and zero (0) in any cell containing the gas phase. Any intermediate value between 0 and 1 would imply that the interface between the phases runs through that cell. The interface tracking is achieved by solving the volume fraction function transport equation of the second phase, which reads as:

$$\frac{\partial}{\partial t}(\alpha_q) + \nabla.(\rho_q \vec{V}_q) \tag{1}$$

where ρ_q represents the density of the secondary phase (or the q^{th} phase) and $\vec{V}_q$ is its velocity vector. In addition to this equation, the flow governing equations are solved for the mixture. The continuity and momentum equation of the following form is used in the current formulation,

$$\frac{\partial \rho}{\partial t} + \nabla.(\rho\, \vec{V}) \tag{2}$$

$$\frac{\partial(\rho\, \vec{V})}{\partial t} + \nabla.(\rho\, \vec{V}) = -\nabla P + \nabla.\left[\mu\left(\nabla \vec{V}\right) + \nabla \vec{V}^T\right] + \rho \tilde{g} \tag{3}$$

The physical properties appearing in the above equations (i.e., ρ and μ) are defined based on the volumetric presence of the constituent phases in each computational cell, expressed as:

$$\rho = \sum_{q=1}^{n} \alpha_q \rho_q \tag{4}$$

$$\mu = \frac{\sum_{q=1}^{n} \alpha_q \rho_q \mu_q}{\sum_{q=1}^{n} \alpha_q \rho_q} \tag{5}$$

The VOF model is thus a kind of a two-phase model which does not consider two immiscible fluids separately. The two fluids are considered a single effective continuum spanning the whole solution domain in this method. The effective fluid's physical properties depend upon the volume fraction's local value, and the interface's motion is then deduced indirectly from these results. It should be noted that coupling between the phases and, subsequently, momentum transfer at the interface is readily achieved through the nature of the VOF method. This formulation is thus simple to implement and computationally economical.

B. Geometric Reconstruction Scheme

In the present simulations, once the interface was captured, a geometric re-construction scheme using a piece-wise-linear (PLIC) approach was used to construct the interface. The interface re-construction scheme explicitly approximates the location of the interface within each cell volume. This is based on the volume fraction values of the cell and its surrounding neighboring cells by allowing the linear interface within each cell to be constructed at an angle to the cell face using the PLIC method. The advection of fluid across the interface cells is computed by assuming a linear slope for each control volume at the interface. The linear slope is given by the

interface normal (gradient of the volume fraction), where the intercept follows from invoking the volume conservation.

After calculating the position of the interface as mentioned above, the amount of fluid convected through each cell is computed using the volume fraction and its derivatives within the cell. The amount of fluid convected through each face is then calculated using the computed linear interface from the previous time step and the normal and tangential velocity components on the cell face. These face volume fluxes are then used in the discretized equations. Further details of the method can be found in Kulkarni [41].

C. Level-set Method Coupling with VOF

The level-set method is one of the popular interface-tracking methods available for two-phase computing flows. Conceptually, this method is similar to the interface tracking method of the VOF model. However, in the method of Osher and Sethian [42], the level-set function is defined as a positive or negative distance from the interface (Γ). One of the strong points of the level-set method is that spatial gradients of the level-set function can be accurately calculated as the function is smooth and continuous. Nevertheless, [43] reported that this method is not volume-conserving.

On the other hand, the VOF method is conservative by nature as it computes and tracks the physical volume fraction in each cell rather than tracking the interface. However, one of the weaknesses of the VOF model is the calculation of the spatial derivatives of the volume-fraction function, which are discontinuous across the interface. The idea of coupling the level-set method and the VOF model is therefore aimed at removing the weaknesses of the two approaches. In the current formulations, the level-set function (φ), can take one of the following values

$$\varphi = \begin{cases} +|d| & \text{primary phase} \\ 0 & \text{Interface} \\ -|d| & \text{secondary phase} \end{cases} \quad (6)$$

Where d represents the distance from the interface Γ. For a two-phase flow system, Γ reads as

$$\Gamma = \{x \,|\varphi(x,t) = 0\} \quad (7)$$

The value of the level-set function throughout the flow domain can then be estimated through the transport equation of the form

$$\frac{\partial \varphi}{\partial t} + \nabla.\left(\vec{V}\varphi\right) = 0 \quad (8)$$

Once the level-set function is estimated, it is used to calculate the normal interface for the VOF re-construction step. This coupling technique was adopted in all the present simulations to improve the accuracy of the interface capture.

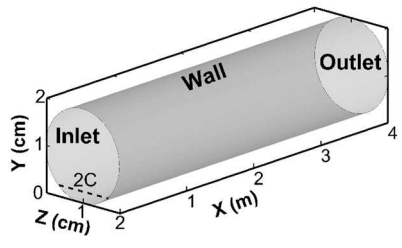

(a)

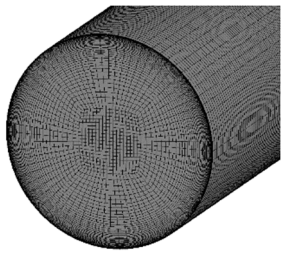
(b)

Fig. 1 (a) Computational domain; (b) Adopted mesh

D. Case Setup

The present simulations were run using a finite-volume pressure-based segregated, implicit solver with the SIMPLE algorithm for the Pressure/Velocity coupling. A 2nd order accurate upwinding scheme was used for the discretization of the convective terms, whereas an implicit time discretization was adopted for all the conservation equations. The details of the suitability of the solver and the numerical discretization procedures have been extensively benchmarked in the past on various configurations [44]–[72].

The Geometric Reconstruction scheme [41], which is used to construct the deformed interface between the phases, requires information about the volume fraction to compute the face fluxes of the volume fraction near the interface. Hence an explicit algorithm was used for the volume fraction equation. For the simulations, a number of eddy viscosity models (EVM) were tested; $k-\varepsilon$, $k-\omega$, and the RNG $k-\varepsilon$ in both standard and differential forms of turbulence viscosity.

The computational domain used for the simulations is shown in Fig. 1a. The chosen domain was scaled down from the experimental setup [9] while preserving both the Reynolds and the Froude numbers. The dimensionalization process is reported in detail in Ali [73]. At the inlet, a mass-flow-rate with a uniform mixture-velocity (normal to the pipe inlet cross-section) was prescribed; the phases were then allowed to develop as the simulations progressed, which settling down naturally to the stratified condition. At the inlet, the mixture turbulence intensity (I) and the turbulence length scales were set to 5% and 0.1D, respectively. A zero gradient outflow boundary condition was employed at the domain exit, whereas both the gas- and liquid-side walls were set as (hydro-dynamically smooth) non-slip solid walls. For all the simulations, the primary phase was considered water, and the second phase was air. The effect of the gravity on the flow was taken into account and the initial flow rates of the mixture along with the volume fractions of the two phases were set to match the inflow conditions.

For all the simulations, the non-dimensional time step was set to give the local *CFL* (Courant Friedrichs Lewy) number of around 1. At each step, several inner iterations were performed for the flow to converge to the desired accuracy, even though this is not a strict requirement as the flow is inherently unsteady in nature.

The main strategy of the present simulations is to automatically capture the interface between the gas and liquid phases (initially set as a homogeneous mixture and flowing co-currently) without any a-priori knowledge about the interface. The flow was allowed sufficient time to firstly separate, and then the liquid-level was allowed to build-up (to

a steady height) as the calculations progressed. The total flow development time was about 10 flow-through passes based on the gas phase superficial velocity. Once the liquid level height in the flow domain was stable (not changing as the solution progressed), a statistical time-averaging of the solution was commenced based on a further 5-10 flow-through passes.

E. Mesh Sensitivity Study

The computational domain comprising of a fully conforming hexahedral mesh with an O-grid topology was generated. At the center of the pipe, a square blocking topology was utilized to avoid skewed cells. A zoomed-in 3-D view of the computational domain is shown in Fig. 1b.

A number of grids with increasing refinement ratios were generated for the mesh sensitivity study (see TABLE I). However, only three grid results are shown here, namely Coarse, Fine, and Finest (see Fig. 2). The grid resolution study was based on refining the mesh in the central section of the O-grid by comparing a number of flow parameters for the different grids. The refinements of the fine and the finest grids were respectively set to 4 and 8 times that of the number of cross-sectional cells in the coarse mesh. Note that a non-dimensional wall distance of $y^+ = 1$ was set for all meshes.

TABLE I
GRID INDEPENDENCE STUDY

Mesh Name	Cells/Cross-section	Gas Bulk Velocity (m/s)	Pressure Gradient (Pa/m)
Coarse	756	0.9730	4.94
Fine	3276	0.9777	1.89
Finest	5952	0.9782	1.78

The grid-independence tests were carried out using the Differential RNG $k-\varepsilon$ model. A summary of some of the numerical results along with the mesh parameters is given in Table1. It was noted that a refinement of 300% resulted in a change of about 62% for the pressure gradient and about 0.5% for the mean gas-phase bulk velocity (area-weighted average of the mean gas velocity over the gas flow cross-section area).

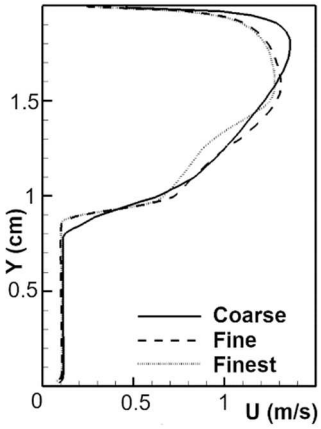

Fig. 2 Mesh Sensitivity Study

A further refinement of approximately 80% resulted in only 5% and 0.05% changes for the mean pressure gradient and the mean gas-phase bulk velocity, respectively. It was thus decided not to refine the mesh any further, and the remaining results are all presented as the finest mesh. Apart from the mean bulk variables, mean velocity profiles at various stations (not reported herein) were also tested for the three grids to ensure that the reported results are grid-independent.

F. Experimental Data

A set of experimental data [9] for the wavy stratified two-phase flow regime in a long horizontal pipe. The measured data has subsequently been used for comparisons with a number of numerical studies; [8], [10].

TABLE II
GLOBAL EXPERIMENTAL VARIABLES

#	Height	V_{SG}	$\langle U_G \rangle$	$\langle U_L \rangle$	$\lvert dp/dx \rvert$	$\langle \tau_G \rangle$	$\langle \tau_L \rangle$	$\langle \tau_i \rangle$
1	42.9	1.2	2.03	0.24	1.65	0.02	0.18	0.04
2	41.0	1.7	2.76	0.25	3.00	0.03	0.16	0.08
3	38.8	3.1	4.83	0.27	6.85	0.09	0.25	0.18
4	34.5	4.3	6.19	0.32	8.70	0.14	0.34	0.21
5	32.5	4.9	6.82	0.35	10.4	0.16	0.43	0.28
6	30.0	5.5	7.35	0.39	13.8	0.18	0.58	0.47
7	26.0	6.6	8.31	0.48	15.5	0.23	0.73	0.55
8	20.5	8.6	10.0	0.67	25.1	0.32	1.35	1.20

Global Experimental Variables from [9]. V_{SG}-Superficial Inflow Gas Velocity (ms^{-1}), $\langle U_G \rangle$-Mean Gas Velocity (ms^{-1}), $\langle U_L \rangle$-Mean Liquid Velocity (ms^{-1}), $|dp/dx|$-Mean Pressure Gradient ($Pam\text{-}1^{1}$). Estimates Done by [8] using [9] Data: $\langle \tau_G \rangle$-Mean Gas phase wall shear stress (Pa), $\langle \tau_L \rangle$-Mean Liquid Phase Wall Shear Stress (Pa) and $\langle \tau_i \rangle$ Mean Interface Shear Stress (Pa)

The measurements [9] were restricted to a fixed liquid flow rate V_{SL} of 0.1 m/s. For brevity, the global experimental variables/results [9] are summarized in TABLE . The reported measurements include the superficial inflow gas velocity ($V_{SG} = Q_G/A$), the mean values of gas ($\langle U_G \rangle$) and water ($\langle U_L \rangle$) velocities and the pressure gradient ($|dp/dx|$). It should be noted here that the original [9] measurements do not report the shear stresses. The last three columns of TABLE , i.e., the wall shear stress for the gas and liquid phases and the shear stress at the interface, $\langle \tau_G \rangle$, $\langle \tau_L \rangle$ and $\langle \tau_i \rangle$ respectively, were estimated [8] through the [9] measurements of the pressure gradients using the momentum balance in each of the two phases.

III. RESULTS AND DISCUSSIONS

A. Hydraulic Gradient (HG)

In two-phase pipe flows, the Hydraulic Gradient (HG) is defined as the drop of liquid phase level over the entire pipe length. At low gas-phase flow rates, the computed liquid levels were found to drop gradually in the flow stream-wise direction. The measurements [9] also show a similar behavior where the hydraulic gradient (HG) was not detected above the inlet superficial gas flow velocity (V_{SG}) of ~2.4 m/s. The computed HGs for the current cases at different V_{SG} are shown by the vertical profiles of the stream-wise velocity at different stream-wise locations ($100D$ and $150D$) along the flow domain in Fig. 3a and b. It was observed that the HG decreases as the V_{SG} increases, reaching to zero for $V_{SG} = 3.1$ m/s.

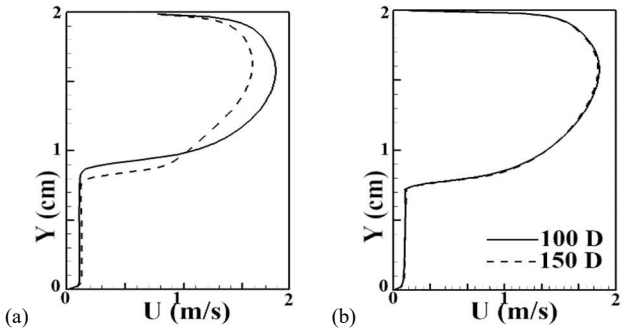

Fig. 3 Effect of Hydraulic Gradient (HG) on the Vertical Profiles of the Stream-wise Velocity at Stream-wise Locations 100D and 150D from the inlet: (a) $\boldsymbol{V_{SG}}$= 1.7 m/s; (b) $\boldsymbol{V_{SG}} = \mathbf{3.1}$ m/s.

The simulations observed that the HG was relatively small ~ 0.045D over a pipe length of 70 D) between locations that were well away (at least 50 D) from both the inlet and outlet of the pipe. [9] also reported an HG of ~0.04 D over a pipe length of 70 D. It should be noted here that the drop in the liquid level becomes slightly sharp close to the flow outlet face (~5-7 D of the pipe length), which is due to the imposed outlet boundary condition. The hydraulic gradient was found to affect the calculated vertical profiles of the time-averaged stream-wise velocity along the flow domain as the flow cross-sectional area changes for each phase. It aims to conserve the mass flow rate. The corresponding stream-wise velocity changes (see Fig. 4). One plausible explanation is that at low gas flow rates, the momentum of the gas phase is not sufficient to sweep the liquid surface. In other words, the momentum transferred by the gas- to the liquid phase is not high enough to accelerate the liquid film and balance the frictional forces between the liquid film and the liquid side wall. Indeed, this argument is supported by the results, as one can observe that as the inflow gas flow rate increases, the hydraulic gradient (HG) disappears. Furthermore, the interfacial waves that start developing at high inlet gas flow rates help stabilize the liquid level as the interfacial waves travel faster than the liquid layer beneath them. Such phenomena have been reported several times but never properly addressed in past experimental or numerical studies.

TABLE III
COMPUTED AVERAGE VELOCITY COMPARISONS WITH EXPERIMENTS

	Experiments [8]	**Current CFD**	**Error %**
U_G/V_{SG}	1.6916 m/s	1.7593 m/s	4.0
U_L/V_{SG}	0.2025 m/s	0.2011 m/s	0.6

B. Turbulence Modelling

For the current simulations, once the numerical solution reached a time-averaged stable condition (i.e., statistically steady), the calculated flow parameters in both phases were analyzed and compared to the corresponding experimental measurements. For the low V_{SG} cases (Fig. 3a), where the hydraulic gradient was observed, the calculated liquid levels at flow cross-sections were monitored at various downstream locations. Once the monitored liquid level stopped changing with time, the obtained flow solution was considered converged. The maximum value of gas-phase stream-wise velocity was also traced along the flow domain. The location at which this maximum velocity (peak velocity) matched the corresponding experimental results was chosen as a plane for post-processing and reporting all of the current results.

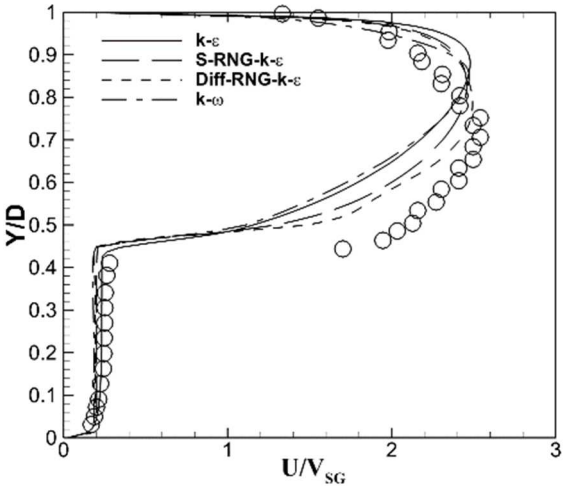

Fig. 4 Comparisons of various turbulence model predictions of the stream-wise velocity along the pipe height at $Z/D = 0.5$ for the $V_{SG} =$ 1.2 m/s case.

Fig. 4 shows the computed profiles of the stream-wise velocity along the vertical center line using different eddy-viscosity turbulence models for the $V_{SG} = 1.2$ m/s case. The presented velocity field is normalized by the gas superficial velocity. It was observed that the velocity profiles of all the turbulence models behaved more or less the same as the Differential RNG $k-\varepsilon$ model, which compared lightly better to the measurements [9].

In the near-wall regions in both phases, all the models predict a similar behavior. This is attributed to the low Reynolds number near wall treatment which is the same for all the models. However, near the interface, especially in the gas phase, none of the models could reproduce the exact experimental profiles. One can observe that on the gas side, there is a slight underprediction of the velocity near the interface, which essentially means that either the predicted turbulent kinetic energy is not high enough or the model is over dissipative.

The standard and differential RNG $k-\varepsilon$ models have additional damping terms for near-wall treatment, where they perform slightly better by reducing the amount of dissipation in the flow, thereby increasing the net turbulent kinetic energy. However, at the interface, all eddy viscosity models should perform the same because they are based on the Boussinesq hypothesis and can thus, not account for the rapid changes in the shear across the interface. It is prudent to mention here that a Reynolds Stress model with low Reynold's treatment was also tested, but the predictions near the interface did not improve. Thus, it is concluded that the large-scale unsteadiness at the interface requires resolution through a truly transient approach such as Large Eddy Simulation (LES).

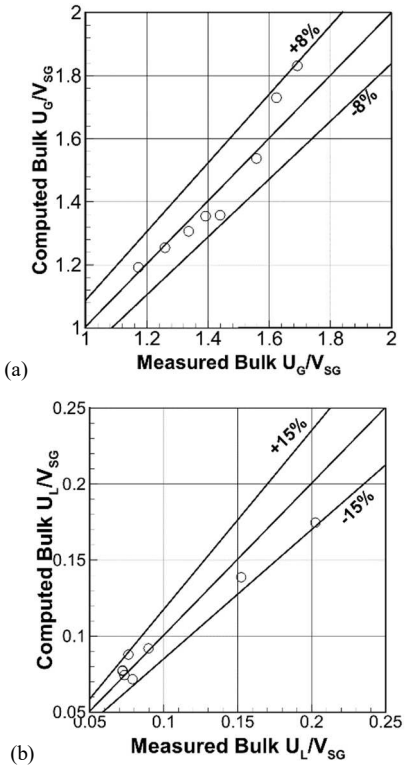

Fig. 5 Comparisons of the mean phase bulk velocity with measurements of [14] (a) Gas phase; (b) Liquid phase

The predicted mean (bulk) velocity of the two phases was also computed and compared with the experiments. These mean bulk phase averaged values were deduced from the solution by averaging the stream-wise velocity of a particular phase over its relative cross-sectional area. For the liquid phase, the best prediction had an error of 0.6% compared to the measurements, whereas for the gas phase, the error was about 4% (see TABLE III). All the models produced similar results, with the Differential RNG $k-\varepsilon$ model performing slightly better. Hence for the remaining sections, only the results from the Differential RNG $k-\varepsilon$ model will be presented.

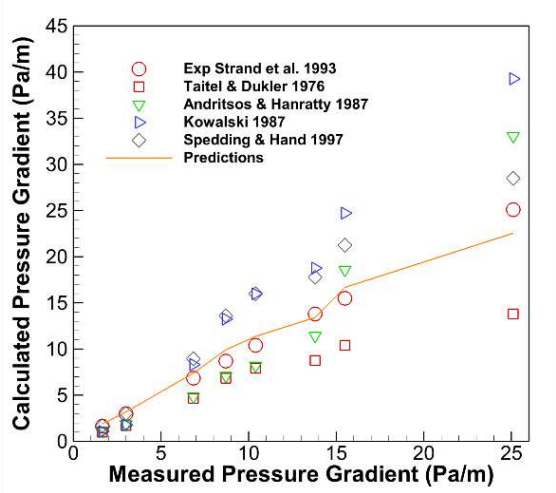

Fig. 6 Stream-wise pressure gradient comparisons between the present simulations, the measured values of [9], and different mechanistic models; [74], [75], [76], [77].

C. Bulk Velocities and Mean Pressure Drop

Compared to the measurements of [9], the computed bulk velocities were found to be within 8% for the gas side and 15% for the liquid side (see Fig. 5). The mean pressure drop in straight horizontal pipes is generally calculated as the sum of the wall and interfacial frictions. For the present simulations, the computed pressure drop was directly obtained by recording the time-averaged static pressure at two different successive points on the top wall ($125D$ & $150D$ from the entrance). For the fully developed stratified steady-state conditions, the pressure is usually measured on the gas side wall [9]. The performance of the present simulations can further be examined by comparing the results of a number of mechanistic models with experiments. Among the many mechanistic models available, the following were used in the present comparisons: [6], [74], [75]. Predictions of the models above were obtained only for the pressure gradient, with the liquid height taken from the reported experimental values. Comparisons of the present simulations were found to be good, as shown in Fig. 6, where the experimental measurements and the CFD predictions almost overlap for the entire range of measured pressure gradients.

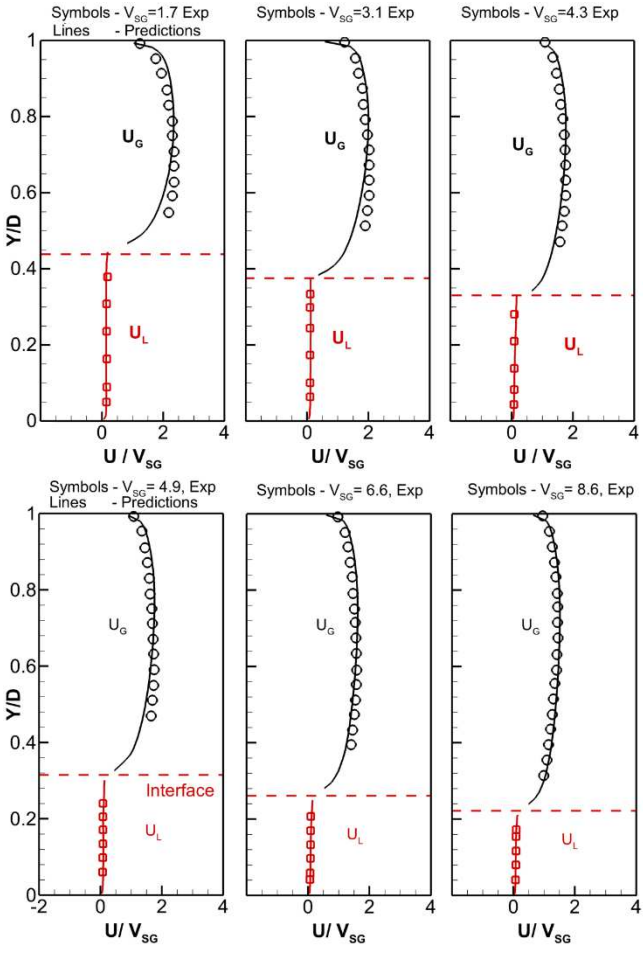

Fig. 7 Normalized stream-wise velocity (U/V_{SG}) comparisons at symmetry plane ($Z/D = 0.5$)

As expected, the predictions [76] were the best amongst the tested mechanistic models as they implicitly include the effect of the increased interfacial roughness and the momentum interactions through additional correlations. It is prudent to

mention here that the predictive accuracy of the different mechanistic models' decreases as the gas flow rate is increased, see the spread of the model predictions, especially at high-pressure gradients in Fig. 6. This is generally related to an increase in interfacial roughness with increasing gas flow rates. The bulk pressure drop results are consistent with this argument, as the figure shows that all models, predictions, and measurements report the same values at low gas flow rates.

D. Vertical Velocity Profiles Across the Interface

Comparisons of the numerical predictions with the measured vertical profiles of the stream-wise velocity along the plane of symmetry ($Z/D = 0.5$) are shown in Fig. 7. It is observed from these plots that near the bottom wall and the liquid side interface, the velocity comparisons are excellent. Furthermore, the gas flow comparisons near the top wall also seem to coincide with the experimental measurements. However, on the gas side, near the interface, especially for the low gas flow rates cases ($V_{SG} = 1.7$ case in particular), the present simulations slightly underpredict the gas velocities (U_G/V_{SG}).

One way of explaining the behavior of the gas phase velocity predictions could be through the comparisons of the boundary conditions between the interface (gas side) and the top wall. If the friction velocity at the interface was equal to the top wall shear stress, one would see a completely symmetrical parabolic profile in the entire gas phase. However, as one would intuitively deduce, the friction at the interface is somewhat lower than at the top wall. This should result in a higher local gas flow velocity at the interface compared to the top wall. However, this is not the case; for the low gas flow cases. One plausible explanation for this is that at the interface, there will be a momentum transfer between the two phases, where the heavier phase, water, will transfer some of its momentum to the gas phase, thus resulting in an increase in the local gas phase velocity at the interface. This certainly seems to be true for the higher gas flow cases ($V_{SG} > 3.1$), where both the experiments and the numerical predictions show similar behavior. For these higher gas flow cases, the interface becomes hydro-dynamically rough, leading to the development of the interfacial waves (ripples in $2 - D$), see the sharp roll-up waves in Fig. 12. It is speculated that these ripples are responsible for the momentum transfer from the liquid to the gas phase. Clearly, this explanation is plausible for the low gas flow cases ($V_{SG} < 3.1$) as well, where there is an absence of the interfacial waves and hence lower velocities at the interface on the gas side.

A simple way of explaining this behavior near the interface would thus be that both the friction and the momentum transfer increase as the gas flow rate increases. However, the rate of increase of friction and momentum transfer is not the same (the increase of momentum rate is much higher than the increase in the interface friction), and since the effect of both these quantities is opposite, one notices an increase in the local velocity near the interface on the gas side. Similar conclusions can be drawn when one looks at the velocity trend (not shown herein) of [8]. However, their measurements are somewhat better near the interface as the authors use measured interfacial shear stress rather than the self-computed ones in the present case.

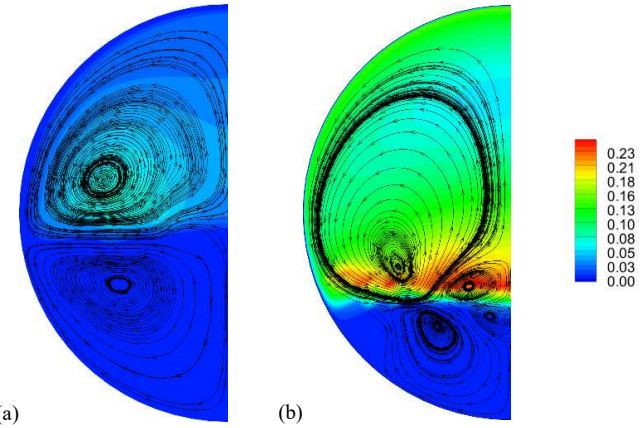

Fig. 8 Calculated turbulent kinetic energy contours in a cross-section superimposed with the flow streamlines showing the secondary flow (only left half of the duct shown due to symmetry). (a) $\boldsymbol{V_{SG} = 1.2}$ m/s (b) $\boldsymbol{V_{SG} = 5.5}$ m/s

E. Secondary Flow and Momentum Transfer

In a two-phase flow such as this one, the mismatch of velocities between the two phases leads to the development of strong secondary flows. Fig. 8 shows the turbulence kinetic energy contours superimposed by the velocity streamlines for two cases; $V_{SG} = 1.2$ & 5.5 m/s.

One can see from this figure that as the mismatch between the two phases increases, i.e., as the inlet gas flow rate increases, the secondary flow becomes much stronger with multiple individual vortices, all directed from the periphery of the pipe towards the interface. These secondary currents, thus, not only generate the interfacial waves but are also responsible for the momentum transfer between the two phases. As seen before, for the lower gas flow case, i.e., $V_{SG} = 1.2$ m/s, the secondary flow is not very strong. Thus, there is limited momentum transfer across the interface and hence low local flow velocities near the interface in the gas region. Similar observations were made regarding the momentum transfer across the interface [8], [78]. It is further observed from the contours of Fig. 8 that the secondary flow not only increases the momentum transfer across the interface but also increases the local roughness. Hence, the local turbulence levels are just above the interface; see the highly energetic turbulent zones just above the interface in Fig. 8. It should be noted here that in contrast to the gas-phase, where the secondary flows are a result of anisotropy of the turbulence, the existence of secondary flows in the liquid-phase is a result of non-linear interaction between the interfacial waves and the mean liquid flow **Error! Reference source not found.**.

F. Horizontal Velocity Profiles & Shear Stresses

Fig. 9 and Fig. 10 show the normalized mean horizontal profiles of the stream-wise velocity (U/V_{SG}) in both the phases. The symmetry of the numerically predicted profiles confirms that the flow has fully developed, and sufficient time averaging has been performed on the statistics. The figures show that for both phases, the velocity predictions are very close to the experimental measurements [9]. Furthermore, at low gas flow rates, one can observe a slight dip in the stream-wise velocity near the symmetry plane (i.e., at $Z/D \approx 0.5$). As the gas flow rate increases, this dip vanishes and the flow

becomes full developed, similar to the vertical velocity profiles of a simple single phase channel flow.

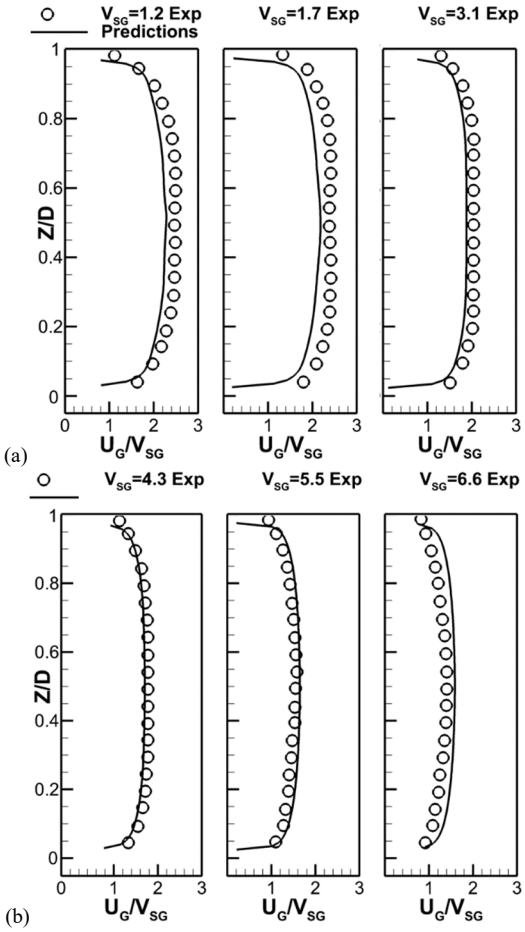

Fig. 9 Normalized stream-wise gas-phase velocity (U_G/V_{SG}) comparisons at $Y/D = 0.65$ location.

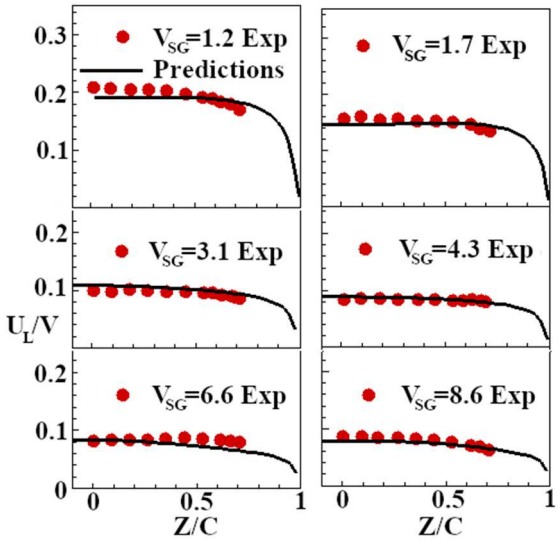

Fig. 10 Normalized stream-wise liquid-phase velocity (U_L/V_{SG})) comparisons at $Y/D = 0.1$ location, where C is the chord length (see Fig. 1).

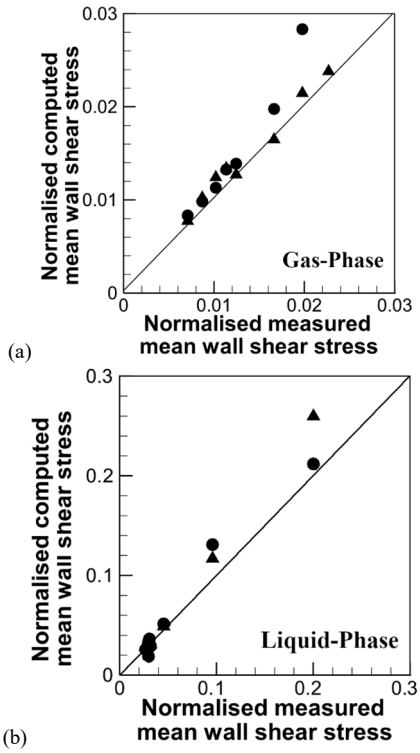

Fig. 11 Normalized mean shear stresses (a) gas-phase wall; (b) liquid-phase wall.

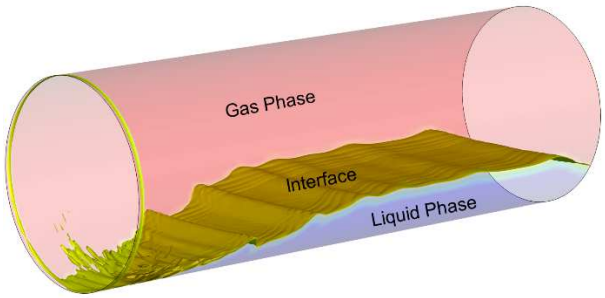

Fig. 12 Isosurfaces of the liquid-gas phases showing the interface and the roll-up waves for a high gas flow rate case.

Comparisons of the shear stress between the current predictions and numerical simulations [8] are shown in Fig. 11. It is observed from Fig. 11b that the average mean wall shear stress at the bottom wall (liquid phase) compares well to the Meknassi et al. [8] data. However, the top wall shear stress in the gas phase is slightly over predicted. Finally, for the interface, the current predictions severely underpredict the interfacial stresses. However, this is partly viewed as a shortcoming of the VOF model but mostly due to the inability of the tested eddy viscosity models to account for the strong shear at the interface between the two phases as pointed out earlier.

IV. Conclusions

The present study provides detailed validations of predictions of a stratified two-phase flow in a pipe using the VOF model. It was shown that the VOF formulation, with the re-construction technique for tracking the interface, was

sufficiently successful in providing good estimates for both the liquid and the gas phases.

For the mean global quantities (velocity and pressure), all mechanistic models and CFD predictions compared quite well for the low inlet gas flow cases. However, the mechanistic model's performance seemed to deteriorate for the high inlet gas flow cases, whereas CFD predictions were still reasonably good. On the other hand, the CFD predictions near the interface on the gas side seemed to be slightly underestimated for the mean local velocity profiles. This deterioration in the predictions was found to be due to the inability of the eddy viscosity (EVM) RANS type turbulence models, which cannot truly account for the flow unsteadiness. The secondary currents generated due to the mismatch of the velocity between the two phases generate the interfacial waves and are responsible for the momentum transfer between them. At low inlet gas flow rates, the EVM's either underestimate the local production or are over dissipative, which causes the local velocities at the gas side interface to be lower than the measurements. The comparisons seem to improve for the higher inlet gas flow rates cases where the strong secondary currents lead to the momentum transfer from the liquid to the gas side.

The VOF model naturally couples the flow field of both the phases through the physical properties of the phases. These physical properties are themselves a function of the captured interface. This means that the predicted velocities around the interface will always be affected by the mixture's physical properties since they are being computed based on the interface rather than the actual physical properties of the original phase. The presented results thus provide a clear picture for the use of mechanistic models and the CFD predictions over a wide range of inlet gas flow rate cases. The presented formulation also differs from the standard techniques in the open literature as it does not require any a-priori empirical information such as the interfacial shear stress or the height of the interface. The presented approach is quite promising when estimating the primary design parameters such as pressure-drop and/or liquid hold-up, and seems to perform better than the industrial mechanistic models, especially for the high gas flow rate cases.

NOMENCLATURE

C	chord length	m
d	distance from the interface	m
dP/dx	pressure gradient in stream-wise direction	Nm^{-3}
q	phase index	-
U	velocity	ms^{-1}
U_G	gas-phase velocity	ms^{-1}
$\langle U_G \rangle$	mean gas-phase velocity	ms^{-1}
U_L	liquid-phase velocity	ms^{-1}
$\langle U_L \rangle$	mean liquid- phase velocity	ms^{-1}
V_{SG}	superficial inflow gas velocity	ms^{-1}

Greek letters

α	phase volume fraction	-
α_q	secondary phase volume fraction	-
Γ	Interface	-
μ_{eff}	effective viscosity	$kgm^{-1}s^{-1}$
μ_q	viscosity of the secondary phase	$kgm^{-1}s^{-1}$
μ_t	turbulent viscosity	$kgm^{-1}s^{-1}$
ν	kinematic viscosity	m^2s^{-1}
ρ_q	density of the secondary phase	kgm^{-3}
$\langle \tau_G \rangle$	mean gas-phase wall shear stress	Nm^{-2}
$\langle \tau_i \rangle$	mean interface shear stress	Nm^{-2}
$\langle \tau_G \rangle$	mean liquid-phase wall shear stress	Nm^{-2}
φ	level-set function	-

Subscripts

i	interface
q	secondary phase
G	gas
L	liquid
SG	superficial gas

Abbreviations

CFD	computational fluid dynamics
EVM	eddy viscosity model
HG	hydraulic gradient
SIMPLE	semi-implicit method for pressure-linked equations
VOF	volume of fluid

REFERENCES

[1] C. H. Newton and M. Behnia, "A numerical model of stratified wavy gas–liquid pipe flow," *Chemical Engineering Science*, vol. 56, no. 24, pp. 6851–6861, 2001.

[2] P. L. Spedding and R. K. Cooper, "A note on the prediction of liquid hold-up with the stratified roll wave regime for gas/liquid co-current flow in horizontal pipes," *International Journal of Heat and Mass Transfer*, vol. 45, no. 1, pp. 219–222, 2002.

[3] G. H. Yeoh and J. Tu, Computational techniques for multi-phase flows. Elsevier, 2010.

[4] R. I. Issa, "Prediction of turbulent, stratified, two-phase flow in inclined pipes and channels," *International Journal of Multiphase Flow*, vol. 14, no. 2, pp. 141–154, 1988.

[5] O. Shoham and Y. Taitel, "Stratified turbulent-turbulent gas-liquid flow in horizontal and inclined pipes," *AIChE Journal*, vol. 30, no. 3, pp. 377–385, 1984.

[6] Y. Taitel and A. E. Dukler, "A model for predicting flow regime transitions in horizontal and near horizontal gas-liquid flow," *AIChE Journal*, vol. 22, no. 1, pp. 47–55, 1976.

[7] C. H. Newton and M. Behnia, "Numerical calculation of turbulent stratified gas-liquid pip flows," *International Jounral of Multiphase Flow*, vol. 2, no. 26, pp. 327–337, 2000.

[8] F. Meknassi, R. Benkirane, A. Liné, and L. Masbernat, "Numerical modeling of wavy stratified two-phase flow in pipes," *Chemical Engineering Science*, vol. 55, no. 20, pp. 4681–4697, 2000.

[9] O. Strand, "An experimental investigation of stratified two-phase flow in horizontal pipes," 1993.

[10] K. Sidi-Ali and R. Gatignol, "Interfacial friction factor determination using CFD simulations in a horizontal stratified two-phase flow," *Chemical Engineering Science*, vol. 65, no. 18, pp. 5160–5169, 2010.

[11] S. C. K. de Schepper, G. J. Heynderickx, and G. B. Marin, "CFD model of all gas-liquid and vapour-liquid flow regimes prpredict by the Baker chart.," *Chemical Engineering Journal*, vol. 138, no. 1, pp. 349–357, 2008.

[12] J. Kou, S. Gong, and W. Yang, "Numerical simulation research on flow pattern of gas-water two-phase flow in horizontal pipeline," in *Mechanic Automation and Control Engineering (MACE), 2011 Second International Conference on*, 2011, pp. 484–487.

[13] Z. Lin, X. Liu, L. Lao, and H. Liu, "Prediction of two-phase flow patterns in upward inclined pipes via deep learning," *Energy*, vol. 210, Nov. 2020, doi: 10.1016/j.energy.2020.118541.

[14] D. Zhang, H. Zhang, J. Rui, Y. Pan, X. Liu, and Z. Shang, "Prediction model for the transition between oil–water two-phase separation and dispersed flows in horizontal and inclined pipes," *Journal of Petroleum Science and Engineering*, vol. 192, Sep. 2020, doi: 10.1016/j.petrol.2020.107161.

[15] R. Kiran, R. Ahmed, and S. Salehi, "Experiments and CFD modelling for two phase flow in a vertical annulus," *Chemical Engineering*

Research and Design, vol. 153, Jan. 2020, doi: 10.1016/j.cherd.2019.10.012.
[16] I. M. Carraretto, L. P. M. Colombo, D. Fasani, M. Guilizzoni, and A. Lucchini, "Pressure Drop and Void Fraction in Horizontal Air–Water Stratified Flows with Smooth Interface at Atmospheric Pressure," *Fluids*, vol. 5, no. 3, Jun. 2020, doi: 10.3390/fluids5030101.
[17] Z. Xu, F. Wu, X. Yang, and Y. Li, "Measurement of Gas-Oil Two-Phase Flow Patterns by Using CNN Algorithm Based on Dual ECT Sensors with Venturi Tube," *Sensors*, vol. 20, no. 4, Feb. 2020, doi: 10.3390/s20041200.
[18] S. Sichamnan, T. Chompookham, and T. Parametthanuwat, "A case study on internal flow patterns of the two-phase closed thermosyphon (TPCT)," *Case Studies in Thermal Engineering*, vol. 18, Apr. 2020, doi: 10.1016/j.csite.2020.100586.
[19] A. H. Zitouni, A. Arabi, Y. Salhi, Y. Zenati, E. K. Si-Ahmed, and J. Legrand, "Slug length and frequency upstream a sudden expansion in gas-liquid intermittent flow," *Experimental and Computational Multiphase Flow*, vol. 3, no. 2, Jun. 2021, doi: 10.1007/s42757-020-0068-0.
[20] S. Ban, W. Pao, and M. S. Nasif, "Numerical simulation of two-phase flow regime in horizontal pipeline and its validation," *International Journal of Numerical Methods for Heat & Fluid Flow*, vol. 28, no. 6, Aug. 2018, doi: 10.1108/HFF-05-2017-0195.
[21] M. G. Conte, G. A. Hegde, M. J. da Silva, A. K. Sum, and R. E. M. Morales, "Characterization of slug initiation for horizontal air-water two-phase flow," *Experimental Thermal and Fluid Science*, vol. 87, Oct. 2017, doi: 10.1016/j.expthermflusci.2017.04.023.
[22] T. Hibiki and S. Rassame, "Analytical model for predicting oil fraction in horizontal oil–water two-phase flow," *Experimental and Computational Multiphase Flow*, vol. 1, no. 1, Mar. 2019, doi: 10.1007/s42757-019-0013-2.
[23] M. Roshani *et al.*, "Evaluation of flow pattern recognition and void fraction measurement in two phase flow independent of oil pipeline's scale layer thickness," *Alexandria Engineering Journal*, vol. 60, no. 1, Feb. 2021, doi: 10.1016/j.aej.2020.11.043.
[24] Y. Chi, C. Sarica, and N. Daraboina, "Experimental investigation of two-phase gas-oil stratified flow wax deposition in pipeline," *Fuel*, vol. 247, Jul. 2019, doi: 10.1016/j.fuel.2019.03.032.
[25] M. S. Shadloo, A. Rahmat, A. Karimipour, and S. Wongwises, "Estimation of Pressure Drop of Two-Phase Flow in Horizontal Long Pipes Using Artificial Neural Networks," *Journal of Energy Resources Technology*, vol. 142, no. 11, Nov. 2020, doi: 10.1115/1.4047593.
[26] Z. Lin, X. Liu, L. Lao, and H. Liu, "Prediction of two-phase flow patterns in upward inclined pipes via deep learning," *Energy*, vol. 210, Nov. 2020, doi: 10.1016/j.energy.2020.118541.
[27] C. Shanthi and N. Pappa, "An artificial intelligence based improved classification of two-phase flow patterns with feature extracted from acquired images," *ISA Transactions*, vol. 68, May 2017, doi: 10.1016/j.isatra.2016.10.021.
[28] A. J. Roman, P. J. Kreitzer, J. S. Ervin, M. S. Hanchak, and L. W. Byrd, "Flow pattern identification of horizontal two-phase refrigerant flow using neural networks," *International Communications in Heat and Mass Transfer*, vol. 71, Feb. 2016, doi: 10.1016/j.icheatmasstransfer.2015.12.033.
[29] L. Liu and B. Bai, "Flow regime identification of swirling gas-liquid flow with image processing technique and neural networks," *Chemical Engineering Science*, vol. 199, May 2019, doi: 10.1016/j.ces.2019.01.037.
[30] E. Khamehchi and A. Bemani, "Prediction of pressure in different two-phase flow conditions: Machine learning applications," *Measurement*, vol. 173, Mar. 2021, doi: 10.1016/j.measurement.2020.108665.
[31] H. Shaban and S. Tavoularis, "Measurement of gas and liquid flow rates in two-phase pipe flows by the application of machine learning techniques to differential pressure signals," *International Journal of Multiphase Flow*, vol. 67, Dec. 2014, doi: 10.1016/j.ijmultiphaseflow.2014.08.012.
[32] Z.-C. Li and C.-L. Fan, "A novel method to identify the flow pattern of oil–water two-phase flow," *Journal of Petroleum Exploration and Production Technology*, vol. 10, no. 8, Dec. 2020, doi: 10.1007/s13202-020-00987-1.
[33] Z. Yang, H. Ji, Z. Huang, B. Wang, and H. Li, "Application of convolution neural network to flow pattern identification of gas-liquid two-phase flow in small-size pipe," Oct. 2017. doi: 10.1109/CAC.2017.8242984.
[34] E. A. Kanin, A. A. Osiptsov, A. L. Vainshtein, and E. V. Burnaev, "A predictive model for steady-state multi-phase pipe flow: Machine learning on lab data," *Journal of Petroleum Science and Engineering*, vol. 180, Sep. 2019, doi: 10.1016/j.petrol.2019.05.055.
[35] M. Chaari, A. C. Seibi, J. ben Hmida, and A. Fekih, "An Optimized Artificial Neural Network Unifying Model for Steady-State Liquid Holdup Estimation in Two-Phase Gas–Liquid Flow," *Journal of Fluids Engineering*, vol. 140, no. 10, Oct. 2018, doi: 10.1115/1.4039710.
[36] M. Ballesteros, N. Ratkovich, and E. Pereyra, "Analysis and Modeling of Liquid Holdup in Low Liquid Loading Two-Phase Flow Using Computational Fluid Dynamics and Experimental Data," *Journal of Energy Resources Technology*, vol. 143, no. 1, Jan. 2021, doi: 10.1115/1.4047604.
[37] A. Khosravi, J. J. G. Pabon, R. N. N. Koury, and L. Machado, "Using machine learning algorithms to predict the pressure drop during evaporation of R407C," *Applied Thermal Engineering*, vol. 133, Mar. 2018, doi: 10.1016/j.applthermaleng.2018.01.084.
[38] G. Mask, X. Wu, and K. Ling, "An improved model for gas-liquid flow pattern prediction based on machine learning," *Journal of Petroleum Science and Engineering*, vol. 183, Dec. 2019, doi: 10.1016/j.petrol.2019.106370.
[39] H. Abbas Khawaja and M. Moatamedi, "Methodology: computational fluid dynamics-discrete element modeling of fluidized beds," in *Multiphysics Modelling of Fluid-Particulate Systems*, Elsevier, 2020. doi: 10.1016/B978-0-12-818345-8.00002-0.
[40] C. W. Hirt and B. D. Nichols, "Volume of fluid (VOF) method for the dynamics of free boundaries," *Journal of Computational Physics*, vol. 39, no. 1, pp. 201–225, 1981.
[41] V. D. Kulkarni, "A piecewise linear interface tracking method for 3-D Eulerian incompressible fluid dlows, Master's thesis," Ottawa, Canada., 1998.
[42] S. Osher and J. A. Sethian, "Fronts propagating with curvature-dependent speed: algorithms based on Hamilton-Jacobi formulations," *Journal of Computational Physics*, vol. 79, no. 1, pp. 12–49, 1988.
[43] E. Olsson, G. Kreiss, and S. Zahedi, "A conservative level set method for two phase flow II," *Journal of Computational Physics*, vol. 225, no. 1, pp. 785–807, 2007.
[44] A. Filippone and I. Afgan, "Orthogonal blade-vortex interaction on a helicopter tail rotor," *AIAA Journal*, vol. 46, no. 6, 2008, doi: 10.2514/1.32690.
[45] N. Abed and I. Afgan, "A CFD study of flow quantities and heat transfer by changing a vertical to diameter ratio and horizontal to diameter ratio in inline tube banks using URANS turbulence models," *International Communications in Heat and Mass Transfer*, vol. 89, 2017, doi: 10.1016/j.icheatmasstransfer.2017.09.015.
[46] N. Abed and I. Afgan, "An extensive review of various technologies for enhancing the thermal and optical performances of parabolic trough collectors," *International Journal of Energy Research*, vol. 44, no. 7, 2020, doi: 10.1002/er.5271.
[47] I. Khurshid and I. Afgan, "Modeling the Effect of CO2 Injection in Oil and Gas Reservoirs of Middle East to Estimate the Formation Damage and Enhanced Oil Recovery," *SSRN*. 2021.
[48] S. Benhamadouche, I. Afgan, and R. Manceau, "Numerical simulations of flow and heat transfer in a wall-bounded pin matrix," *Flow, Turbulence and Combustion*, vol. 104, no. 1, pp. 19–44, 2020.
[49] I. Afgan, C. Moulinec, and D. Laurence, "Numerical simulation of generic side mirror of a car using large eddy simulation with polyhedral meshes," *International Journal for Numerical Methods in Fluids*, vol. 56, no. 8, 2008, doi: 10.1002/fld.1719.
[50] K. M. Guleren, I. Afgan, and A. Turan, "Predictions of turbulent flow for the impeller of a NASA low-speed centrifugal compressor," *Journal of Turbomachinery*, vol. 132, no. 2, 2010, doi: 10.1115/1.3140824.
[51] Z. Wu, D. Laurence, and I. Afgan, "Direct numerical simulation of a low momentum round jet in channel crossflow," *Nuclear Engineering and Design*, vol. 313, 2017, doi: 10.1016/j.nucengdes.2016.12.018.
[52] I. Afgan, Y. Kahil, S. Benhamadouche, and P. Sagaut, "Large eddy simulation of the flow around single and two side-by-side cylinders at subcritical Reynolds numbers," *Physics of Fluids*, vol. 23, no. 7, 2011, doi: 10.1063/1.3596267.
[53] X. Han, P. Sagaut, D. Lucor, and I. Afgan, "Stochastic response of the laminar flow past a flat plate under uncertain inflow conditions," *International Journal of Computational Fluid Dynamics*, vol. 26, no. 2, 2012, doi: 10.1080/10618562.2012.655687.
[54] Z. Wu, D. Laurence, H. Iacovides, and I. Afgan, "Direct simulation of conjugate heat transfer of jet in channel crossflow," *International Journal of Heat and Mass Transfer*, vol. 110, 2017, doi: 10.1016/j.ijheatmasstransfer.2017.03.027.

[55] Y. Kahil, S. Benhamadouche, A. S. Berrouk, and I. Afgan, "Simulation of subcritical-Reynolds-number flow around four cylinders in square arrangement configuration using LES," *European Journal of Mechanics, B/Fluids*, vol. 74, 2019, doi: 10.1016/j.euromechflu.2018.11.008.

[56] Z. Wu, D. Laurence, S. Utyuzhnikov, and I. Afgan, "Proper orthogonal decomposition and dynamic mode decomposition of jet in channel crossflow," *Nuclear Engineering and Design*, vol. 344, 2019, doi: 10.1016/j.nucengdes.2019.01.015.

[57] P. T. L. Nguyen, J. C. Uribe, I. Afgan, and D. R. Laurence, "A Dual-Grid Hybrid RANS/LES Model for Under-Resolved Near-Wall Regions and its Application to Heated and Separating Flows," *Flow, Turbulence and Combustion*, vol. 104, no. 4, 2020, doi: 10.1007/s10494-019-00070-8.

[58] A. E. A. Ali, I. Afgan, D. Laurence, and A. Revell, "A dual-mesh hybrid RANS-LES simulation of the buoyant flow in a differentially heated square cavity with an improved resolution criterion," *Computers and Fluids*, vol. 224, 2021, doi: 10.1016/j.compfluid.2021.104949.

[59] Y. Kahil, S. Benhamadouche, A. S. Berrouk, and I. Afgan, "Simulation of subcritical-Reynolds-number flow around four cylinders in square arrangement configuration using LES," *European Journal of Mechanics - B/Fluids*, vol. 74, pp. 111–122, 2019.

[60] U. Ahmed, D. Apsley, T. Stallard, P. Stansby, and I. Afgan, "Turbulent length scales and budgets of Reynolds stress-transport for open-channel flows; friction Reynolds numbers (Re_τ) = 150, 400 and 1020," *Journal of Hydraulic Research*, pp. 1–15, 2020.

[61] I. Afgan, S. Benhamadouche, X. Han, P. Sagaut, and D. Laurence, "Flow over a flat plate with uniform inlet and incident coherent gusts," *Journal of Fluid Mechanics*, vol. 720, 2013, doi: 10.1017/jfm.2013.25.

[62] U. Ahmed, D. D. Apsley, I. Afgan, T. Stallard, and P. K. Stansby, "Fluctuating loads on a tidal turbine due to velocity shear and turbulence: Comparison of CFD with field data," *Renewable Energy*, vol. 112, 2017, doi: 10.1016/j.renene.2017.05.048.

[63] N. Abed, I. Afgan, A. Cioncolini, H. Iacovides, and A. Nasser, "Assessment and Evaluation of the Thermal Performance of VariousWorking Fluids in Parabolic Trough Collectors of Solar Thermal Power Plants under Non-Uniform Heat Flux Distribution Conditions," *Energies*, vol. 13, no. 15, 2020, doi: 10.3390/en13153776.

[64] C. Ejeh, I. Afgan, R. Shittu, A. Sakirudeen, and P. Anumah, "Investigating the impact of velocity fluctuations and compressibility to aerodynamic efficiency of a fixed-wing aircraft," *Results in Physics*, vol. 18, 2020, doi: 10.1016/j.rinp.2020.103263.

[65] U. Ahmed, D. Apsley, T. Stallard, P. Stansby, and I. Afgan, "Turbulent length scales and budgets of Reynolds stress-transport for open-channel flows; friction Reynolds numbers R <inf> eτ</inf> = 150, 400 and 1020," *Journal of Hydraulic Research*, vol. 59, no. 1, 2021, doi: 10.1080/00221686.2020.1729265.

[66] P. T. L. Nguyen, J. C. Uribe, I. Afgan, and D. R. Laurence, "A dual-grid hybrid RANS/LES model for under-resolved near-wall regions and its application to heated and separating flows," *Flow, Turbulence and Combustion*, vol. 104, pp. 835–859, 2020.

[67] I. Afgan, J. McNaughton, S. Rolfo, D. D. Apsley, T. Stallard, and P. Stansby, "Turbulent flow and loading on a tidal stream turbine by LES and RANS," *International Journal of Heat and Fluid Flow*, vol. 43, 2013, doi: 10.1016/j.ijheatfluidflow.2013.03.010.

[68] J. Mcnaughton, I. Afgan, D. D. Apsley, S. Rolfo, T. Stallard, and P. K. Stansby, "A simple sliding-mesh interface procedure and its application to the CFD simulation of a tidal-stream turbine," *International Journal for Numerical Methods in Fluids*, vol. 74, no. 4, 2014, doi: 10.1002/fld.3849.

[69] N. Abed, I. Afgan, A. Cioncolini, H. Iacovides, A. Nasser, and T. Mekhail, "Thermal performance evaluation of various nanofluids with non-uniform heating for parabolic trough collectors," *Case Studies in Thermal Engineering*, vol. 22, 2020, doi: 10.1016/j.csite.2020.100769.

[70] I. Khurshid, E. W. Al-Shalabi, I. Afgan, and H. Al-Attar, "A numerical approach to investigate the impact of acid-asphaltene sludge formation on wormholing during carbonate acidizing," *Journal of Energy Resources Technology, Transactions of the ASME*, vol. 144, no. 6, 2022, doi: 10.1115/1.4051738.

[71] C. Ejeh *et al.*, "Computational fluid dynamics for ameliorating oil recovery using silicon-based nanofluids and ethanol in oil-wet reservoirs," *Energy Reports*, vol. 6, 2020, doi: 10.1016/j.egyr.2020.10.028.

[72] A. Revell *et al.*, "Coupled Hybrid RANS-LES Research at The University of Manchester," *ERCOFTAC Bulletin*, vol. 120, p. 67, 2020.

[73] I. T. M. Ali, "CFD Prediction of Stratified and Intermittent Gas-Liquid Two-Phase Turbulent Pipe Flow Using RANS," 2017.

[74] N. Andritsos and T. J. Hanratty, "Influence of interfacial waves in stratified gas-liquid flows," *AIChE Journal*, vol. 33, no. 3, pp. 444–454, 1987.

[75] J. E. Kowalski, "Wall and interfacial shear stress in stratified flow in a horizontal pipe," *AIChE Journal*, vol. 33, no. 2, pp. 274–281, 1987.

[76] P. L. Spedding and N. P. Hand, "Prediction in stratified gas-liquid co-current flow in horizontal pipelines," *International Journal of Heat and Mass Transfer*, vol. 40, no. 8, pp. 1923–1935, 1997.

[77] Y. Taitel and A. E. Dukler, "A theoretical approach to the Lockhart-Martinelli correlation for stratified flow," *International Journal of Multiphase Flow*, vol. 2, no. 5, pp. 591–595, 1976.

[78] M. Nordsveen, "Wave-and turbulence-induced secondary currents in the liquid phase in stratified duct flow," *International Journal of Multiphase Flow*, vol. 27, no. 9, pp. 1555–1577, 2001.